RESISTANCE SPOT WELDING OF MAGNESIUM ALLOY AZ61

T. KRAMAR[1], P. VONDROUS[1], M. KOLARIKOVA[1]
K. KOVANDA[1], L. KOLARIK[1], M. ONDRUSKA[2]
[1]Czech Technical University in Prague
Faculty of Mechanical Engineering in Prague
Prague, Czech Republic
[2]Slovak University of Technology in Bratislava
Faculty of Materials Science & Technology in Trnava
Trnava, Slovak Republic

e-mail: tomas.kramar@fs.cvut.cz

Resistance spot welding (RSW) was used to weld Mg alloy AZ61A. To research weldability of this alloy many welding parameters, e.g. current, time, pressure, have been tried in wide range on the welding source DALEX PMS 11 – 4. Visual check was followed with metallography, tensile test etc. Some defects as solidification, liquation cracks, porosity were found. The creation of imperfections was found to be dependent on parameters, so finally optimized parameters were found. The best influence on weld integrity, i.e. weld w/o cracks, was to set cooling time directly after welding. For sheet metal of 1 mm optimum welding parameters were 8 kA, 100 ms, 9 kN and long cooling time. Another problem found, was limited lifetime of Cu electrodes, when in contact with Mg melt. This contamination damaged surface quality of electrodes, further influencing weld quality. High enough electrode pressure can diminish this problem.

KEYWORDS
resistance spot welding, RSW, Mg alloy, AZ61
solidification cracking

1. INTRODUCTION

Economical use of energy sources, lower emissions and as little as possible harmful impact of modern lifestyle on the environment is now one of main aims of technical development. In aerospace and automotive industries there is wider and wider use of light alloys and materials with high ratio of strength to weight. For example in automotive we can notice wide usage of high strength steels and Al alloys. In aerospace, even lower density than that of Al alloys is looked for, so Magnesium alloys are often the choice. Actually the future is in Mg alloys and it is already used in many automotive, aerospace and other products. Different properties of some metals are shown in Table 1. Mechanical properties of pure metals-Mg, Ti, Al, Fe [Kramar 2014], [Turna 2012].

Mg alloys are prospective material, e.g. in area of transportation, where decrease of weight is a must. Yet especially for structures subjected to dynamic loading, the demands on quality of weldments are very high. One of technologies used for welding car body is Resistance Spot Welding (RSW). Even though weldability of steels and Al alloys by RSW is well known, it cannot be directly applicable on Mg alloys, so the aim of this article is to research weldability of AZ61 by RSW.

1.1. Weldability of Mg alloys

There are some properties of Mg alloys influencing weldability negatively, as strong tendency to oxidize, high thermal conductivity, high coefficient of thermal expansion, low melting and boiling temperatures, wide solidification temperature range, high solidification shrinkage, formation of low melting point constituents, low viscosity, low surface tensions, high solubility for hydrogen in the liquid state, and absence of colour change at the melting point temperature [Turna 2011].

Therefore, weld defects were observed in welding of magnesium alloys by different methods such as unstable weld pool, spatter [Haferkamp 2001], tendency to drop through, sag of the weld pool, undercut, porous oxide inclusions, loss of alloying elements, excessive pore formation [Zhao 2001], liquation and solidification cracking.

Hot cracks have been one of the main welding defects for magnesium alloys. In most magnesium alloys, an increase in alloying elements will generally increase the solidification temperature range. The large freezing temperature range, large solidification shrinkage, high coefficient of thermal expansion, and low melting point intermetallic constituents potentially make magnesium alloys susceptible to heat affected zone liquation cracking and solidification cracking in FZs [Marya 2002]. Solidification cracking usually occurs in the alloys with large solidification interval, such as Mg–Zn–Zr, Mg–Al–Zn, etc. In addition, a number of magnesium alloys are thought to be susceptible to stress corrosion cracking. Thus, the welded joints should be used after stress relieving [Cao 2006].

The alloys containing up to 6 % Al and up to 1 % Zn possess good weldability, while the alloys containing over 6 % Al and up to 1 % Zn are moderately crack sensitive, because of the occurrence of low melting-point constituents ($Mg_{17}Al_{12}$) [Marya 2002]. A frequency of both types of cracks increased at low welding speeds and was associated with high heat input and tensile stress. The experimental observations indicate that for MIG welding of magnesium alloys a reduction in the heat input reduces the frequency of cracks in WM, HAZ.

It was also found that cracking behaviour depend on the grain size and β-$Mg_{17}Al_{12}$ precipitates and liquation cracking can be suppressed by grain refinement. [Chen 2013]

1.2. RSW Weldability

In many of RSW spot welds cracks and pores have been found, affecting the properties of weld. It is caused by high coefficient of linear expansion, the rapid expansion at heating up, followed by quick cool down. The refined fusion-zone microstructure results in a longer fatigue life than welds with a coarse fusion-zone microstructure, when interfacial failure across fusion zone occurs at a higher level of cyclic load range [Xiao 2011].

Weldability of AZ31 was distinctly different from AZ91 as proved by [Luo 2011]. Solidification and liquation cracks in WM and HAZ were found for AZ31, for all welds with diameter over 6.5 mm, high heat input deteriorated the cracking. AZ91D was prone to porosity in WM and weld surface. Even partial contact of Cu electrode with molten Mg diminished electrode life [Kolarikova 2013].

With increasing the current, the weld nugget size increases, yet also the porosity volume and size. This tendency can be counteracted by increase in the electrode force. At sufficiently high electrode force the porosity almost disappears (3–4 kN for AZ31). Also application of holding time

	Mg	Al	Ti	Fe
Thermal capacity ($J.kg^{-1}.K$)	1360	1080	540	795
Heat of fusion ($J.kg^{-1}$)	3.7×10^{5}	4×10^{5}	4.2×10^{5}	2.7×10^{5}
Melting temperature (°C)	650	660	1 666	1536
Boiling temperature (°C)	1090	2520	3 287	2860
Thermal conductivity ($W.m^{-1}.K^{-1}$)	78	94,03	20	38
Thermal coefficient ($m^2.s^{-1}$)	3.73×10^{-5}	3.65×10^{-5}	5.0×10^{-6}	6.80×10^{-6}
Coefficient of thermal expansion (K^{-1})	25×10^{-6}	24×10^{-6}	$8,5\times10^{-6}$	10×10^{-6}
Density ($kg.m^{-3}$)	1590	2385	4506	7015
Resistivity ($\mu\Omega.m$)	0.274	0.2425	0.420	1.386

Table 1. Mechanical properties of pure metals-Mg, Ti, Al, Fe [Kramar 2014], [Turna 2012]

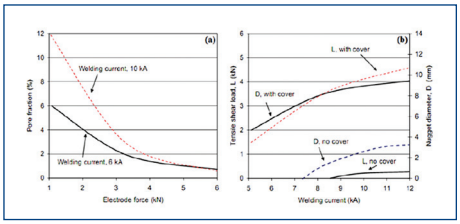

Figure 1. Dependence of porosity and nugget size on parameters [Shi 2010]

after current shut-off caused the reduction in pore formation. Proved was the relative importance of holding time after current shut-off (i.e. cooling time) depends on welding current. [Shi 2010]

Aim of this research is thus to examine weldability of AZ61, to prove influence of contact pressure, cooling time on suppressing hot cracks and increasing strength of the weld.

2. EXPERIMENTAL

2.1 Material

Rolled sheets of alloy AZ61A thick 1 mm were used in all experiments. Chemical and mechanical properties are stated below.

Elements	Al	Zn	Mn	Si	Fe	Ca	Cu	Fe	Mg
Wt. %	6.37	0.67	0.21	0.01	0.004	0.005	0.0005	0.004	Bal.

Table 2. Chemical composition of AZ61A

Rp 0,2 [MPa]	Rm [MPa]	A [%]	Hardness [HV 0,1]
217	271	15	51 – 61

Table 3. Mechanical properties AZ61A

AZ61A consists of 2 phases–delta phase, i.e. solid solution and beta phase –eutectic Mg17Al12 precipitate. Precipitates of beta phase are 3x harder than delta phase. After casting, welding, these are at grain boundaries, so Mg alloys should undergo heat treatment to improve properties. At Figure 3 matrix of delta phase with fine intermetallics (black dots) is visible.

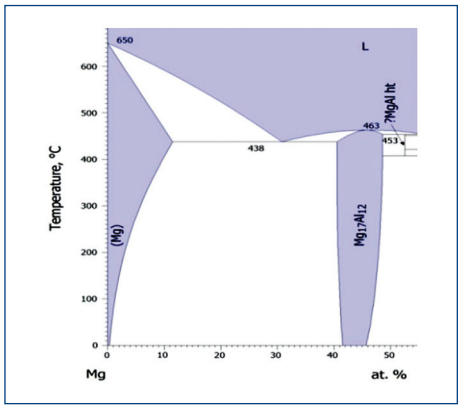

Figure 2. Binary diagram Mg-Al

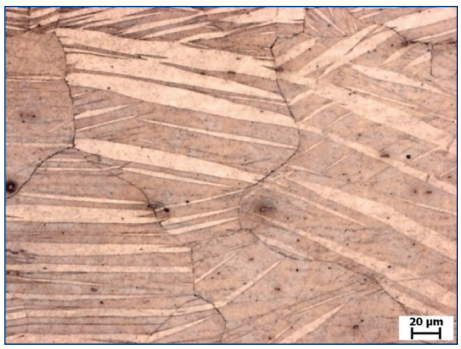

Figure 3. Microstructure of AZ61A

Figure 4. Welding source Dalex

2.2 Welding procedure, welding source, sample

As welding source Dalex PMS 11–4 with range of usable welding parameters – welding time 0–2.5 s, welding current 0–30 kA, electrode force 0.2–10 kN cooling time 0-2.5 s. Cooling time means that electrodes are still in contact after current is switched off. Used electrode caps are 39D 1978-1, mat. CuCr1Zr. [Kolarik 2014]

As welding sample square sheet metal 25x25x1 mm were prepared. For the tensile test samples were 100 x 25 x 1 mm.

2.3 Weld evaluation

Microscopic observation of weld surface and metallography were used to evaluate presence of weld imperfections.

Tensile tests were executed on welded samples. Microhardness was measured.

3. RESULTS

Varying parameters as welding current, welding time, force, preheat and post heat, many different welds were done and evaluated.

3.1 Current, welding time, electr. force

Heat input in RSW is defined by $Q = I^2*R*t$, so current and pulse length are the main welding parameters to set on the source.

In the previous research, time, current influence, welding time on weld size was observed. From the previous experience, current in range 7–9 kA, time 100 ms were selected as giving good nugget size.

Electrode force was changed in range 1–9 kN and results are shown at Figure 6. Increase of contact pressure decreases the size of weld nugget. Probably this is connected with decrease of contact interface resistance with increase of external pressure, thus lower heat input. At the lowest contact force, pressure, 1 kN, the internal pressure of

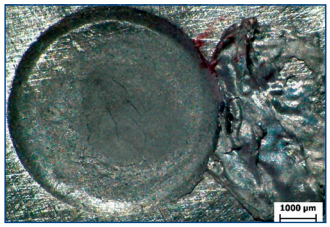

Figure 5. Spot weld upper view, spatter, cracks present 1 kN, 8 kA, t=100 ms, cooling 2.5 s

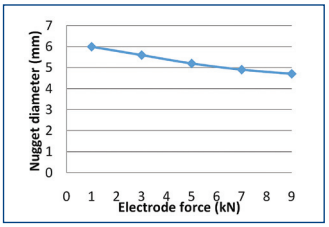

Figure 6. Influence of electr. force on weld nugget diameter, const. I= 8 kA, t=100 ms, cooling time 2.5 s

melt was higher than external electrode force, so that melt ejected and spatter was created, upper view at Figure 5. Due to high thermal expansion of Mg the spatter creation must be suppressed by high enough electrode force. Due to the fact of size changing with the electrode force, the spot loading capacity will change. Influence on microstructure should also be expected.

3.2 Microstructure

Example of microstructure at higher magnification shows presence of fine grain structure, average grain size is 5–10 µm with presence of secondary intermetallic phase at the grain boundaries. This is eutectic intermetallic phase $Mg_{17}Al_{12}$, as stated by other researchers; this is well visible at Figure 7, 8 together with cracking presence.

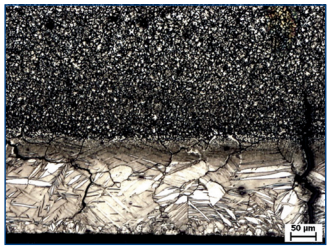

Figure 7. Typical fine grain structure, crack in WM, HAZ

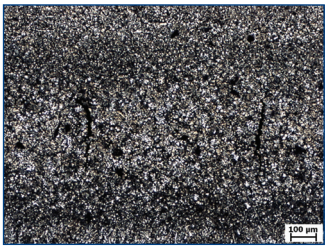

Figure 8. Porosity, solidification cracks visible in the weld nugget

3.3 Cracking

Due to visual check of micrographs on microscope cracks have been found. The cracks typically run along the grain boundaries. These were present in WM near the weld centre and also in HAZ. Characteristics show these are solidification and liquation cracks. This fact is in concordance with other researchers, as stated in chapter Weldability of Mg alloys.

Cracking countermeasures

Hot cracking behaviour, noted at our spot welds, is connected with solidification of weld metal and/or liquation in HAZ.

Generally to prevent hot cracking heat input should be minimized, to minimize volume solidification time, volume of molten metal and segregation. Also in some cases preheat and postheat can help, influencing final weld structure. To observe possibility to prevent solidification cracks, this was tried: 1. Minimizing heat input, 2. Use of cooling time, (after welding electrodes are kept in contact with weld).

1. Minimizing heat input

Even at low welding parameters, the small solidification cracks could be found. Furthermore lower heat input would decrease weld area, size of nugget and possible load.

2. Use of cooling time

If after welding the electrodes are kept in contact with the spot weld, the piece is faster cooled and solidification process finishes faster, thus lowering segregations and cracking. This is proven by comparison of weld done with cooling time 2.5 s, Figure 10, where no cracks were noticed. On the other hand on Figure 9 many cracks near the weld centre, part that solidified the last, were visible.

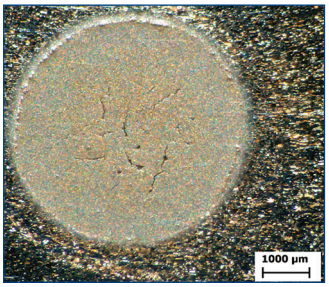

Figure 9. Transversal cross section of the lap weld 8 kA, 100 ms, cooling time 1 s, porosity, cracks visible near the centre

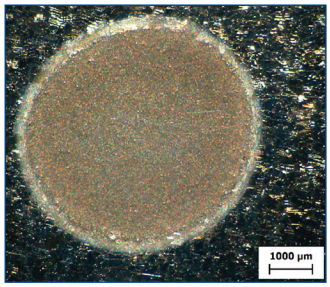

Figure 10. Transversal cross section of the lap weld 8 kA, 100 ms, cooling time 2.5 s, no visible cracks or pores

Too high welding parameters

In case of setting too high parameters, i.e. heat input, the melting of upper or/and lower sheet metal surface can occur. In such case, the melt can be expulsed from weld nugget causing spatter and wetting of the Cu electrode. Contact of molten Mg and Cu electrode causes constant deterioration of electrode surface, i.e. electrode wear. Damaged electrode surface will indent on any further spot welds, as on Figure 12. Melting of Cu electrode and its influence on weld is visible at Figure 11.

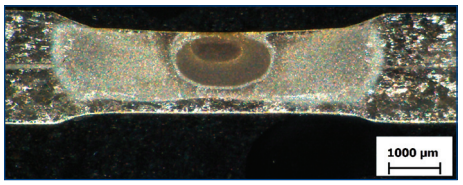

Figure 11. Cross section, lap weld, 8 kA, 100 ms, post heat 2.7 kA, 5 s, Cu presence visible in WM

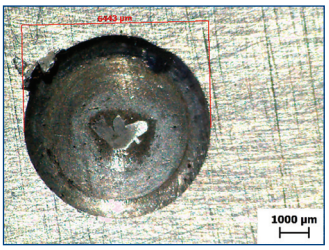

Figure 12. Upper view of spot weld electrode damage indentation

Microhardness

Vickers microhardness was measured according to norm ČSN EN ISO 14271 on machine Buehler IndentaMet 1106 with load of 100 g. Distance of indentations was 0.5 mm.

Increase of hardness was noticed in WM for all samples. Example of results can be visible at Figure 13. Base metal hardness was on average 57 HV0.1. The highest average WM hardness was 67 HV0.1 for, measured for 9 kN, while for force of 1 kN it was 61 HV0.1. The increase of hardness in WM is connected with recrystallization under outer pressure, causing grain refinement. The change of microhardness with change of electrode force is quite significant.

Shear test

To evaluate strength of weld joints shear test (in accordance with ČSN EN ISO 14273) was applied using tensile testing machine LABORTECH LabTest 5.150 Sp1. Test samples were prepared at welding current 9 kA, time 0,1 s, force 1, 3, 5, 7, 9 kN. For each set of parameters 5 samples were prepared. One sample was subjected to tensile test to find tensile strength of BM, for which the max load was 5316 N.

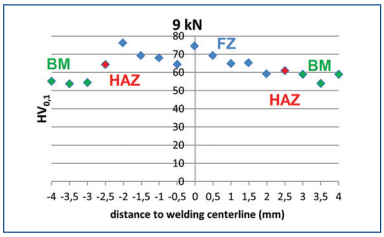

Figure 13. Hardness across weld nugget, I= 8 kA, t=100 ms, 9 kN, cooling 2,5 s

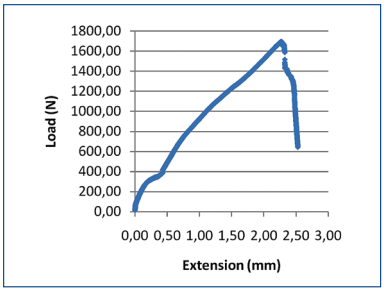

Figure 14. Shear test load-extension graph

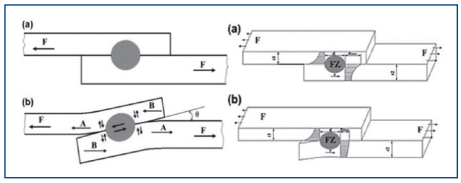

Figure 15. Forces (left), shear stresses (right). At the moment of a–start of test, b–during execution [Zhang 2013]

Forces applied on shear test sample cause distortion of sample, as visible at Figure 15, so direct comparison of BM sample and test samples is not possible because of characteristics of lap weld.

All samples fractured outside from the weld metal, so the welds can be evaluated as acceptable, visible at Figure 16a. The highest loads at the fracture were reached for the highest electrode force, i.e. 7,9 kN. This is probably connected with increase of joint soundness, as this diminishes porosity and cracks. Results are visible at Figure 16 b.

4. CONCLUSION

RSW weldability of AZ61 was researched with following conclusions: solidification and/or liquation cracks (microcracks) along grain boundaries are to be expected. Their presence can be diminished by minimizing solidification time, e.g. lowering heat input, setting cooling time. That was done in our case, when after welding electrodes were kept in contact with weld spot for 2.5 s, i.e. cooling time, then the cracking was not observed.

In the shear test all samples fractured outside of WM. The shear test proved that increase of electrode force increases also maximum load. For dynamic loading the presence of porosity and cracks should be evaluated with more details.

The influence of electrode force upon weld nugget size and spatter was contrary to our expectations, as increase of contact pressure decreased size of the weld nugget and prevented spatter. Decrease of nugget size can be explained by decrease of contact resistance, by higher applied force, consequently heat input. As the conclusion, the cooling time and higher electrode force proved advantageous for welding of AZ61 to suppress cracking and increase strength of the joint.

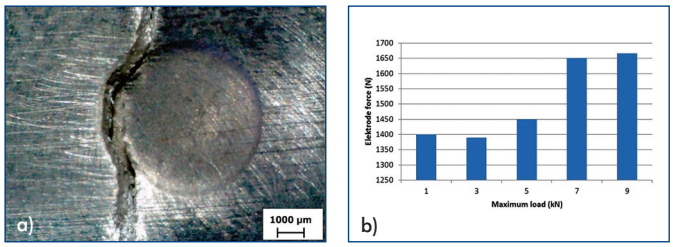

Figure 16. Shear test: a) fracture of test specimen, b) Results of shear test

ACKNOWLEDGMENT

This research was supported by the grant SGS 13/187/OHK 2/3T12.

REFERENCES

[Cao 2006] Cao, X. et al. A review of laser welding techniques for magnesium alloys. Journal of Materials Processing Technology, 2006, 171.2:188-204.

[Chen 2013] Chen, X. L., Yan, H. G., Chen, J. H., Su, B., Yu, Z. H. Effects of grain size and precipitation on liquation cracking of AZ61 magnesium alloy laser welding joints. Science and Technology of Welding and Joining, Volume 18, Issue 6, August 2013

[Haferkamp 2001] Haferkamp, H. et al. Laser beam welding of magnesium alloys – new possibilities using filler wire and arc welding. Proc LANE: Laser Assist Net Shape Eng, 2001.

[Kolarik 2014] Kolarik, L., Sahul, M., Kolarikova, M., Sahul, M., Turna, M. Resistance spot welding of low carbon steel to austenitic CrNi stainless steel. In: Advanced Materials Research. Zurich: Trans Tech Publications, Ltd., 2014, p. 1499-1502. ISSN 1022-6680. ISBN 978-3-03785-993-3.

[Kolarikova 2013] Kolarikova, M., Kolarik, L.The influence of resistence spot welding on weld joint quality and service life of elektrodes In: Conference METAL 2013 Proceedings. Ostrava: Tanger spol. s r. o., 2013, p. 766-771. ISBN 978-80-87294-41-3.

[Kramar 2014] Kramar, T. Welding of Mg alloys by selected welding methods [Dissertation Thesis], STU in Bratislava. MTF in Trnava. Thesis supervisor: doc. Dr. Ing. Pavel Kovacocy – Trnava: MTF STU, 2014. 180 s.

[Luo 2011] Luo, B. H., Hao, C., Zhang, J., Gan, Z., Chen, H., Zhang, H. Characteristics of Resistance Welding Magnesium Alloys AZ31 and AZ91. In: Welding Journal, 90, s. 249 – 257. ISSN 0043-2296, 2011.

[Marya 2002] Marya, M., Edwards, G. R. Influence of laser beam variables on AZ91D weld fusion zone microstructure. Science and technology of welding and joining, 2002, 7.5: 286-293.

[Shi 2010] Shi, H.Effects of welding parameters on the characteristics of magnesium alloy joint welded by resistance spot welding with cover plates.Materials & Design, 2010, 31.10: 4853-4857.

[Turna 2011] Turna, M., Ondruska, J., Sahul, M., Kupec, T., Kramar, T., Turnova, Z. Trends in welding of Mg alloys. (in Slovak) In: XXXIX. International conference Welding 2011 (Zvaranie 2011),2011, p. 1-10. ISBN 978-80-89296-14-9.

[Turna 2012] Turna, M., Turnova, Z., Ondruska, J., Sahul, M., Kupec, T., Kramar T. Welding of Mg alloys. (in Slovak) In: Strojarstvo-Strojirenstvi, 2012, Vol. 16, n. 4 p. 36-39. ISSN 1640-3622

[Xiao 2011] Xiao, L. et al. Resistance spot weld fatigue behavior and dislocation substructures in two different heats of AZ31 magnesium alloy.Materials Science and Engineering: A, 2011, 529: 81-87.

[Zhang 2013] Zhang, H. et al. Failure analysis of dissimilar thickness resistance spot welded joints in dual – phase steels during tensile shear test AZ31 and AZ91. In: Material & Design, 2013, 55, s. 366 – 372. ISSN 0261-3069

[Zhao 2001] Zhao, H., Debroy, T. Pore formation during laser beam welding of die-cast magnesium alloy AM60B-mechanism and remedy. Welding Journal, 2001, 80.8.

CNTACTS

Ing. Tomas Kramar, PhD.
Department of Manufacturing Technology
Faculty of Mechanical Engineering CTU in Prague
Technicka 4, 166 07 Prague, Czech Republic
tel.: +420 224 352 630
e-mail: tomas.kramar@fs.cvut.cz